



Poly(ethylene glycol)-based ammonium ionenes containing nucleobases

Mana Tamami, Sean T. Hemp, Keren Zhang, Mingqiang Zhang, Robert B. Moore, Timothy E. Long*

Macromolecules and Interfaces Institute, Department of Chemistry, Virginia Tech, Blacksburg, VA 24061, USA

ARTICLE INFO

Article history:

Received 14 November 2012

Received in revised form

24 January 2013

Accepted 27 January 2013

Available online 1 February 2013

Keywords:

Segmented ionenes

Nucleobases

¹H NMR titration

ABSTRACT

Adenine-functionalized ionenes (ionene-A) and thymine-functionalized ionenes (ionene-T) were synthesized from novel nucleobase-containing monomers from an efficient aza-Michael addition to an acrylate precursor. Complexes of ionenes with nucleobase-containing guest molecules (*n*-butyl thymine, *n*BT and *n*-butyl adenine, *n*BA) exhibited well-defined complementary hydrogen bonding interactions. Job's analysis revealed a 1:1 stoichiometry for the hydrogen-bonded complexes of [ionene-A]:[*n*BT], [ionene-T]:[*n*BA], and [*n*BA]:[*n*BT]. A mathematical fit of the chemical shifts to the Benesi–Hildebrand method revealed the association constants of 94 M⁻¹, 130 M⁻¹, and 137 M⁻¹ for complexes of [ionene-A]:[*n*BT], [ionene-T]:[*n*BA], and [*n*BA]:[*n*BT], respectively. Furthermore, DSC thermograms of 1:1 [ionene-A/T]:[guest molecule] complexes showed the disappearance of the melting transition for the guest molecule, confirming the absence of macrophase separation of the nucleobase guest in the polymer matrix. Morphological studies including atomic force microscopy (AFM) and small-angle X-ray scattering (SAXS) revealed a microphase-separated morphology for the nucleobase-containing ionenes and less defined microphase separation for the 1:1 complexes.

© 2013 Elsevier Ltd. All rights reserved.

1. Introduction

Future advances in polymer design will involve the use of non-covalent interactions, such as hydrogen bonding, electrostatics, π – π interactions, metal coordination, and Van der Waals forces to develop supramolecular polymers for diverse applications. DNA exquisitely utilizes both complementary hydrogen bonding with nucleobases and ionic interactions and many polymer scientists draw inspiration from DNA to synthesize nucleobase-containing structures [1]. Environmental stimuli including temperature, solvent polarity, humidity, concentration, and pH readily control the strength of these interactions, thus leading to responsive polymers [2].

Ionenes are ion-containing polymers that contain quaternized nitrogens in their backbone [3]. The quantitative step-growth polymerization of a ditertiary amine with a dihalide monomer produces families of ionenes. Typical monomers include dimethyl amines and alkyl chlorides to ensure a quantitative polymerization process for high molecular weights. The synthetic strategy provides control over charge density and placement, and consequently ionenes are ideal models to investigate structure–property relationships of well-defined cationic polymers. Due to the positive

charge of ammonium ionenes, they are versatile in many biomedical applications such as gene transfection agents [4,5], cosmetics [6], antimicrobial agents [7], and flocculants for water treatment [8].

Two general families of ionenes are segmented and non-segmented copolymers with various topologies. Segmented [9] ionenes have oligomeric, low T_g spacers between their charged sites and demonstrate enhanced mechanical properties compared to non-segmented [10] ionenes, which generally contain shorter alkylene spacers between charges and therefore higher charge density along the backbone. In this manuscript, we report segmented 1000 g/mol poly(ethylene glycol) (PEG)-based ionenes that contain pendant adenine or thymine units. The PEG segment enhances polymer solubility in organic solvents and increases chain mobility compared to non-segmented ionenes, leading to desirable complementary hydrogen bonding interactions.

Previous literature describes a wide variety of synthetic polymers functionalized with complementary adenine and thymine nucleobases or with nucleobase mimics [11–17]. However, few reports detail the incorporation of complementary hydrogen bonding in the presence of ionic interactions. Rotello et al. [18] used orthogonal self-assembly of polymers and nanoparticles to micro-pattern surfaces. However, the hydrogen bonding recognition units and charged species resided on separate polymer backbones. Weck et al. [19] synthesized ammonium and 2,6-diaminopyridine (DAP)-functionalized norbornene diblock copolymers containing both

* Corresponding author.

E-mail address: telong@vt.edu (T.E. Long).

electrostatic and hydrogen bonding interactions. They concluded from ^1H NMR titrations that the non-covalent interactions were orthogonal, and electrostatics did not disrupt hydrogen bonding. Recently, Hemp et al. [20] copolymerized 9-vinylbenzyladenine (VBA) and 2-(dimethylamino)ethyl methacrylate (DMAEMA) with subsequent protonation to provide adenine-containing polyelectrolytes. Copolymers having 11, 22, and 35 mol% of VBA showed polyelectrolyte behavior in dilute and semidilute regimes. Due to the hydrogen bonding association between adenine units, they did not observe polyelectrolyte behavior in the concentrated regime. In addition, the electrospinning behavior showed a strong dependence on the VBA incorporation. We also demonstrated the interplay between hydrogen bonding and electrostatic interactions in both solid and solution states with poly(9-vinylbenzyladenine-*b*-*n*-butyl acrylate-*b*-9-vinylbenzyladenine) triblock copolymers and selective association of uracil-containing salts with adenine units [21].

We report the synthesis and characterization of water-soluble, adenine (A) and thymine (T) functionalized (K_{AT} ca. 100 M^{-1} in CDCl_3) segmented poly(ethylene glycol) (PEG)-based ammonium ionenes for supramolecular assembly. Supramolecular assembly studies between the adenine and thymine nucleobases probed the influence of electrostatics on complementary hydrogen bonding. In the solution state, ^1H NMR titration studies determined the stoichiometry as well as association constants, K_a , between adenine- and thymine-containing PEG-ionenes with complementary guest molecules. In the solid state, we investigated the effect of self-complementary hydrogen bonds and complementary hydrogen bonds on thermal and morphological properties of adenine- and thymine-ionenes as well as their complexes with guest molecules.

2. Experimental

2.1. Materials

3,3-Iminobis(*N,N*-dimethylpropylamine) (DMPA, 97%), acryloyl chloride (97%), 6-bromohexanoyl chloride (97%), and triethylamine (TEA, 99%) were purchased from Aldrich and vacuum distilled prior to use. Potassium tert-butoxide (99.99%), adenine (A, 99%), thymine (T, 99%), poly(ethylene glycol) (PEG) with $M_n = 1000 \text{ g/mol}$, sodium bicarbonate (99.7%), magnesium sulfate (99.5%), 1-bromobutane (99%), and potassium carbonate (>99%) were obtained from Sigma–Aldrich and used without further purification. γ -butyrolactone (+99%) and diisobutylaluminum hydride (1.0 M solution in toluene) were purchased from Aldrich and used as received. Dichloromethane (DCM, HPLC grade), tetrahydrofuran (THF, HPLC grade), and dimethyl formamide (DMF, HPLC grade) were passed through alumina and molecular sieve columns before use. Chloroform (CHCl_3 , HPLC grade) and ethyl acetate (EtOAc, HPLC grade) were purchased from Fischer Scientific and used as received.

2.2. Instrumentation

^1H NMR spectroscopic analyses were performed on Varian Advance 500 MHz spectrometer to confirm monomer and polymer compositions at ambient temperature in CDCl_3 or CD_3OD . Fast Atom Bombardment Mass Spectrometry (FAB-MS) was conducted in positive ion mode on a JEOL HX110 dual focusing mass spectrometer. Differential scanning calorimetry (DSC) was conducted on a TA Instruments Q100 under a nitrogen flush of 50 mL/min at a heating rate of $10^\circ\text{C}/\text{min}$. The glass transition temperatures were measured as the midpoint of the transition in the second heating scan. Thermogravimetric analysis (TGA) was conducted on a TA Instruments Hi-Res TGA 2950 under nitrogen at a heating rate of $10^\circ\text{C}/\text{min}$. Atomic force microscopy (AFM) was performed using a Veeco MultiMode (Veeco Instruments, Plainview, NYA). AFM was

equipped with Nanosensor silicon tips having a spring constant of 42 N/m . Samples were imaged at a set-point ratio of 0.70 with a magnification of $1 \mu\text{m} \times 1 \mu\text{m}$. SAXS was performed using a Rigaku S-Max 3000 3 pinhole SAXS system, equipped with a rotating anode emitting X-ray with a wavelength of 0.154 nm ($\text{Cu K}\alpha$). Scattering from a Silver behenate standard was used to calibrate the sample-to-detector distance. For SAXS, the sample-to-detector distance was 1603 mm. Two-dimensional SAXS patterns were obtained using a fully integrated 2D multiwire, proportional counting, gas-filled detector, with an exposure time of 1 h. All SAXS data were analyzed using the SAXSGUI software package to obtain radically integrated SAXS intensity versus scattering vector q (SAXS), where $q = (4\pi/\lambda)\sin(\theta)$, θ is one half of the scattering angle and λ is the wavelength of X-ray profiles.

2.3. Synthesis of *N,N*-bis(3-(dimethylamino)propyl)-4-hydroxybutanamide

The acrylic monomer was synthesized using two steps. In the first step, a flame-dried, 2000-mL, three-neck, round-bottomed flask was attached to a 250-mL addition funnel and a condenser. The round-bottomed flask was charged with 50 mL (1.00 mol) of 3,3-iminobis(*N,N*-dimethylpropylamine) and 700 mL tetrahydrofuran (THF). The round-bottomed flask was purged with nitrogen. Diisobutylaluminum hydride (1.0 M solution in toluene, 225 mL, 1.00 mol) was added to the addition funnel and subsequently added to the reaction flask in a drop-wise fashion. The solution was stirred for 7 h at 0°C . Subsequently, the reaction flask was warmed to room temperature and 17 mL (1.00 mol) of γ -butyrolactone was added to the reaction mixture and the solution was refluxed for 12 h. Water (10 mL) was added slowly to the cooled reaction flask and THF was evaporated under reduced pressure. A 15% sodium hydroxide solution (100 mL) was added and stirred for an hour. The aqueous layer was extracted three times with 100 mL dichloromethane and the organic fractions were combined. The solvent was concentrated *in vacuo* and the product was purified using Kugelrohr distillation. An overall yield of 70% was obtained. ^1H NMR (500 MHz, CDCl_3): 1.71 (m, 4H, H_c), 1.90 (m, 2H, H_f), 2.21 (d, 12H, H_a), 2.26 (t, 4H, H_b), 2.52 (t, 2H, H_e), 3.35 (m, 4H, H_d), 3.67 (t, 2H, H_g), 3.45 (s, 1H, H_i). HRMS (ES+): m/z calcd for $[\text{M} + \text{H}^+]$ 273.24 g/mol, found 274.17 g/mol (Fig. S1).

2.4. Synthesis of 4-(bis(3-(dimethylamino)propyl)amino)-4-oxobutyl acrylate

In the second step, a flame-dried, 100-mL, round-bottomed flask was connected to a 50-mL addition funnel and was charged with dichloromethane (DCM) and 1.00 eq of hydroxyl-containing tertiary amine monomer that was synthesized from the first step. The flask was cooled to 0°C and acryloyl chloride (1.20 eq) was added to the addition funnel containing DCM and the solution was added drop-wise to the reaction flask. The reaction was allowed to proceed for 12 h. Upon reaction completion, DCM was evaporated and the salt was dissolved in a mixture of saturated NaHCO_3 (aq) and saturated Na_2CO_3 (aq). The aqueous solution was extracted six times with DCM. The solution was concentrated *in vacuo* and the product was purified using Kugelrohr distillation. A yellow oil with an overall yield of 30% was obtained. ^1H NMR (500 MHz, CDCl_3): 1.68 (m, 4H, H_c), 2.02 (m, 2H, H_f), 2.19 (d, 12H, H_a), 2.24 (t, 4H, H_b), 2.42 (t, 2H, H_e), 3.31 (m, 4H, H_d), 4.20 (t, 2H, H_g), 5.78–5.83 (m, 1H, H_{j1}), 6.05–6.14 (m, 1H, H_k), 6.35–6.42 (m, 1H, H_{j2}) (Fig. S2).

2.5. Synthesis of bromine end-capped PEG (Br-PEG-Br)

The commercially available 1000 g/mol poly(ethylene glycol) (PEG) (10 g, 1.00 mol) was introduced to a 250-mL, two-neck, round-bottomed flask equipped with a magnetic stir bar, addition

funnel, and nitrogen inlet. Anhydrous dichloromethane (100 mL) was added to the round-bottomed flask and 50 mL was added to the addition funnel. The flask was cooled to 0 °C and 6-bromohexanoyl chloride (2.20 eq) was added to the addition funnel with a syringe and subsequently added to the reaction flask in a drop-wise fashion. The reaction was allowed to proceed for 24 h. Upon reaction completion, the reaction mixture was washed twice with saturated NaHCO₃ (aq) and twice with distilled water. The DCM layer was separated and dried over magnesium sulfate. The solution was concentrated *in vacuo* and dried under vacuum at 100 °C for 12 h (97% yield). The ¹H NMR number-average molecular weight was 1300 g/mol. The ¹H NMR (400 MHz, CDCl₃) spectroscopy for the bromine end-capped 1K PEG is as follows: δ = 1.47 ppm (m, 4H, per chain, H_c), 1.65 ppm (m, 4H, H_d), 1.87 ppm (m, 4H, H_b), 2.35 ppm (t, 4H, H_e), 3.40 ppm (t, 4H, H_a), 3.64 ppm (m, 76H, H_h), 3.69 ppm (m, 4H, H_g), 4.22 ppm (m, 4H, H_f) (Fig. S3).

2.6. Synthesis of *n*-butyl thymine (*n*BT) guest molecule

Thymine (10.05 g, 80.0 mmol), potassium carbonate (11.06 g, 80.0 mmol), 1-bromobutane (3.67 g, 26.8 mmol), and DMSO (200 mL) were added to a 500-mL round-bottomed flask. The solution was heated to 50 °C for 8 h and then cooled. The resulting precipitate was removed through filtration and the DMSO solution was added to 600 mL water. The aqueous solution was extracted four times with 100 mL DCM and then the organic layer was washed four times with 300 mL water. The organic layer was dried over magnesium sulfate and then concentrated *in vacuo* to obtain a solid. The solid product was recrystallized from chloroform:hexanes to obtain a white solid with a yield of 51%. ¹H NMR (400 MHz, CDCl₃): 0.95 ppm (t, 3H, H_a), 1.36 ppm (m, 2H, H_b), 1.66 ppm (p, 2H, H_c), 1.92 ppm (s, 3H, H_e), 3.69 ppm (t, 2H, H_d), 6.97 ppm (s, 1H, H_f), 8.65 ppm (s, 1H, H_g) (Fig. S4).

2.7. Synthesis of *n*-butyl adenine (*n*BA) guest molecule

Adenine (6.05 g, 44.8 mmol), 1-bromobutane (6.16 g, 45.0 mmol), potassium carbonate (8.33 g, 60.3 mmol), and DMSO (60 mL) were added to a 250-mL round-bottomed flask. The resulting solution was stirred for 48 h at 23 °C and then poured into 600 mL water. The aqueous solution was extracted three times with 100 mL DCM and then the organic layer was washed three times with 100 mL water. The organic layer was dried over magnesium sulfate and concentrated *in vacuo* to obtain a solid. The product was obtained as a white solid after recrystallization from chloroform:hexanes. ¹H NMR (400 MHz, CDCl₃): 0.96 ppm (t, 3H, H_a), 1.37 ppm (m, 2H, H_b), 1.88 ppm (p, 2H, H_c), 4.20 ppm (t, 2H, H_d), 5.67 ppm (s, 2H, H_e), 7.79 ppm (s, 1H, H_f), 8.37 ppm (s, 1H, H_g) (Fig. S5).

2.8. Synthesis of acrylate-containing PEG-based ionene precursor

Upon the synthesis of acrylic ditertiary amine monomer and bromine end-capped PEG, a 1:1 ratio of monomers was polymerized in DMF for 24 h at 80 °C in the presence of a catalytic amount of BHT. The polymer was stored in the DMF solution until the next synthetic step. ¹H NMR (400 MHz, CD₃OD): 1.42 (m, 4H, H_m), 1.72 (m, 4H, H_n), 1.81 (m, 4H, H_i), 2.05 (m, 6H, H_d), 2.40 (m, 4H, H_p), 2.55 (t, 2H, H_e), 3.11 (d, 12H, H_a), 3.33–3.47 (m, 8H, H_{b+c}), 3.50 (t, 4H, H_g), 3.63 (s, 75H, H_{k1+k2}), 3.69 (t, 4H, H_l), 4.18–4.27 (m, 6H, H_f), 5.88–5.93 (dd, 1H, H_{j2}), 6.13–6.22 (m, 1H, H_h), 6.36–6.42 (dd, 1H, H_{j1}) (Fig. S6).

2.9. Synthesis of nucleobase-containing PEG-based ionene using post-polymerization functionalization

After polymerization, the acrylic ionene solution in DMF was charged with 1.20 mol of adenine or thymine and 0.30 mol of

tBuOK for 4 d. The nucleobase-containing ionene product was precipitated in ethyl acetate and dried *in vacuo* (0.1 mmHg) for 24 h (90% yield). ¹H NMR (400 MHz, CD₃OD) for adenine-containing ionene: 1.42 (m, 4H, H_m), 1.70 (m, 4H, H_n), 1.81 (m, 4H, H_i), 1.91 (p, 2H, H_{d'}), 2.06 (m, 4H, H_d), 2.30 (t, 2H, H_e), 2.40 (m, 4H, H_p), 3.01 (t, 2H, H_h), 3.12 (d, 12H, H_a), 3.33–3.59 (m, 8H, H_{b+c+g}), 3.63 (s, 70H, H_{k1+k2}), 3.69 (t, 4H, H_l), 4.15 (t, 2H, H_q), 4.20 (m, 4H, H_f), 4.52 (m, 2H, H_j), 8.16 (s, 1H, H_s), 8.22 (s, 1H, H_r). ¹H NMR (400 MHz, CD₃OD) for thymine-containing ionene: 1.44 (m, 4H, H_m), 1.71 (m, 4H, H_n), 1.81 (m, 4H, H_i), 1.86 (s, 3H, H_s), 1.95 (p, 2H, H_{d'}), 2.08 (m, 4H, H_d), 2.32 (t, 2H, H_e), 2.40 (t, 4H, H_p), 2.77 (t, 2H, H_h), 3.13 (d, 12H, H_a), 3.34–3.59 (m, 8H, H_{b+c+g}), 3.63 (s, 70H, H_{k1+k2}), 3.69 (t, 4H, H_l), 4.00 (t, 2H, H_q), 4.17 (t, 2H, H_j), 4.20 (t, 4H, H_f), 7.49 (s, 1H, H_r) (Fig. S7).

2.10. Preparation of ionene blend with guest molecules

The segmented adenine-containing ionene and thymine-containing ionene solutions in chloroform were mixed with *n*BT and *n*BA chloroform solutions in a 1:1 molar ratio, respectively. The blends were stirred for an hour, and cast in Teflon® molds. Chloroform slowly evaporated at room temperature for 48 h and the films were annealed at 100 °C for 24 h *in vacuo*.

3. Results and discussion

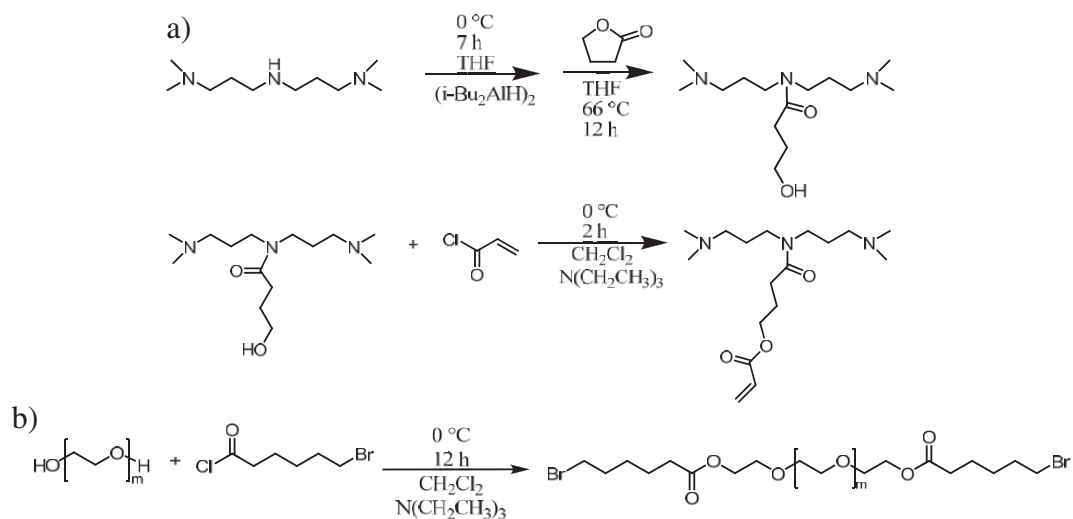
3.1. Synthesis of nucleobase-functionalized PEG-based ionene homopolymers

Synthesis of nucleobase functional PEG-based ionenes involved the synthesis of an acrylic ditertiary amine monomer and an oligomeric bromine-terminated PEG spacer. In the first synthetic step of the acrylic monomer synthesis, the secondary amine ring-opened γ -butyrolactone in the presence of DIBAL, an efficient amidating agent for the conversion of lactones to amides [22]. Thus, the reaction produced an OH-containing ditertiary amine monomer in high yields. In the second step, reaction between the primary alcohol and acryloyl chloride yielded an acrylic ditertiary amine monomer (Scheme 1a). Difunctional bromine-terminated PEG was synthesized in a similar fashion to earlier (Scheme 1b) bromine end-capped poly(propylene glycol) oligomers, and MALDI-TOF mass spectroscopy and titration analysis confirmed their difunctionalities [9].

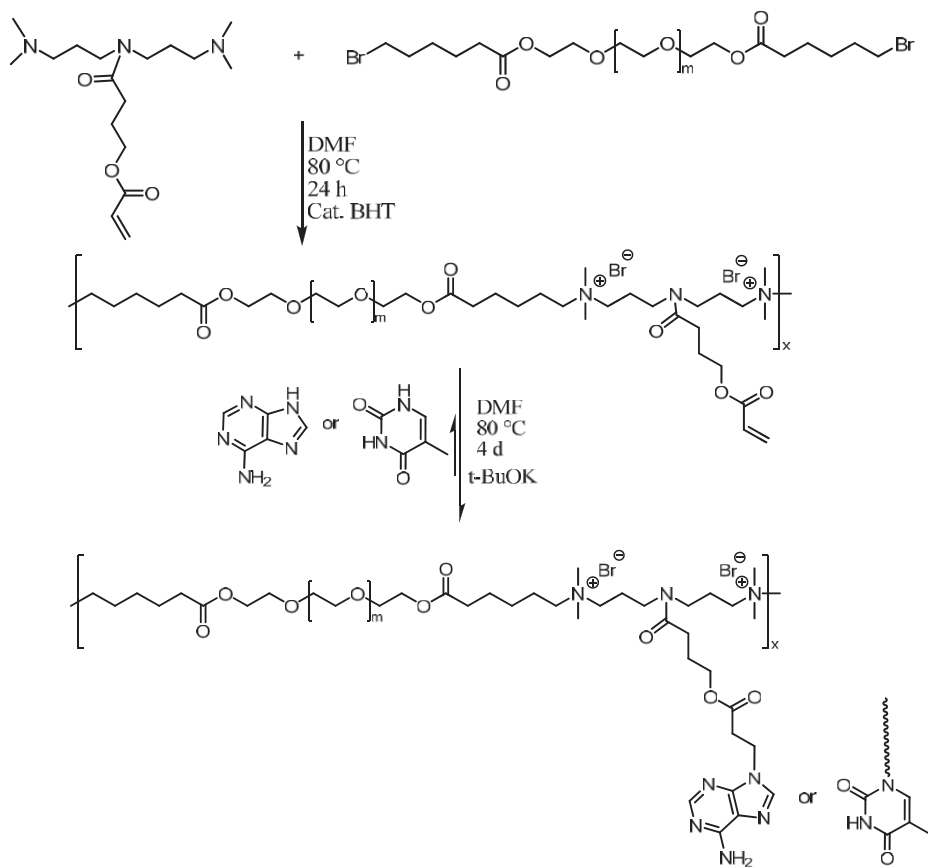
As shown in Scheme 2, the pure, difunctional tertiary amine and bromide monomers reacted according to Menshutkin reaction conditions to provide an acrylate-containing PEG-based ionene. Post-polymerization functionalization without isolation of the precursor using base-catalyzed Michael addition to the acrylate ionene precursor in DMF yielded the adenine-containing ionene (ionene-A) and thymine-containing ionene (ionene-T). The Michael addition reaction solution initially was heterogeneous and became homogeneous upon reaction due to the enhanced solubility of the final nucleobase ionene. The thermodynamically controlled, base-catalyzed Michael addition promoted a regioselective substitution of adenine and thymine at the N9 and N1 positions, respectively. [23] Optimization of the reaction conditions, such as solvent, temperature, and base, resulted in regioselective nucleobase-containing ionenes. ¹H NMR spectroscopy confirmed successful incorporation of the heterocyclic bases, and disappearance of the olefinic protons at 5.8–6.6 ppm confirmed quantitative addition of the nucleobases to the acrylate ionene precursor.

3.2. ¹H NMR titrations

When adenine and thymine nucleobases form complementary hydrogen bonds, the chemical shift for the NH (thymine) and NH₂



Scheme 1. Synthesis of acrylic tertiary amine monomer (a) and bromine end-capped 1000 g/mol PEG (b).



Scheme 2. Post-polymerization functionalization of PEG-based ionene.

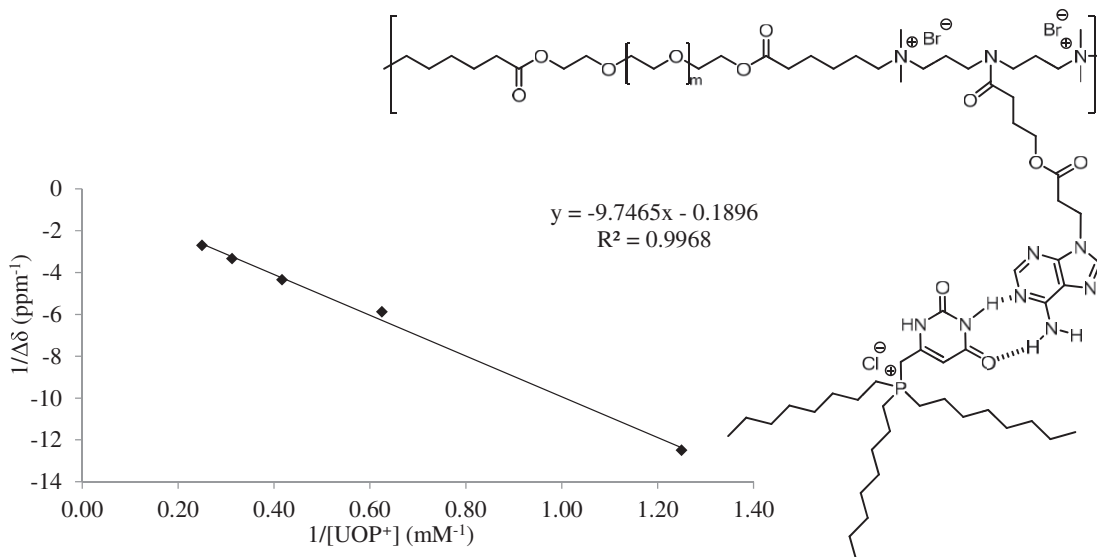


Fig. 1. Benesi–Hildebrand plot of ionene-A and UOP⁺ guest molecule association in CDCl₃.

(adenine) protons shift downfield relative to their original peak position [24]. We blended a 1:1 molar ratio of [ionene-A]:[ionene-T] at a 4 mM nucleobase in chloroform to investigate the formation of complementary multiple hydrogen bonds. However, ¹H NMR resonances of NH and NH₂ protons for the [ionene-A]:[ionene-T] blend had insignificant change in their chemical shifts compared to the ionene homopolymers. In order for the pendant nucleobases to interact, both PEG-based ionene chains must be in close proximity. Due to the charged nature of the ionene backbone and steric hindrance between two bulky nucleobase-containing PEG chains, the formation of a hydrogen bond between the complementary nucleobases was presumably restricted. In order to examine the influence of charge and bulkiness of complementary nucleobases, uracil octyl phosphonium salt (UOP⁺) served as a complementary, low molar mass charged guest molecule for the [ionene-A]. For each repeat unit, the charge ratio of [ionene-A] to [UOP⁺] was 2:1. Therefore, the charge density per repeat unit decreased, and the bulkiness of the complementary nucleobase decreased with a low molecular weight guest molecule compared to high molecular weight PEG ionene. Solutions of [ionene-A]:[UOP⁺] complexes were prepared where the [ionene-A] concentration remained constant at 4 mM and the [UOP⁺] concentration systematically increased. The position of the NH₂ resonance of ionene-A in the complex shifted downfield (from 6.27 to 6.64 ppm) with the increase in [UOP⁺] concentration. The association constant (*K*_a) based on Benesi–Hildebrand plot (Fig. 1) was 19 M⁻¹, which was in acceptable range (10–100 M⁻¹), however, the value was low compared to the neutral guest molecules. Although charge–charge repulsion reduced the strength of association between complementary bases, less sterically hindered guest molecule promoted hydrogen bonding interactions. Thus, we synthesized neutral adenine and thymine-containing small guest molecules to examine the supramolecular assembly of the low molar mass nucleobase guests with the nucleobase ionenes. These guest molecules have low molar mass (190 g/mol), without charge, and the guests are highly soluble in chloroform, which makes them ideal candidates for interaction with the complementary ionene homopolymers.

The stoichiometry of the host–guest complex was necessary before calculating their association constant (*K*_a) [25]. Job's analysis, a continuous variation method, elucidated the host–guest stoichiometry using ¹H NMR spectroscopy [26,27]. Solutions containing

host nucleobase ionenes and low molar mass nucleobase guests were prepared in chloroform. The total solution concentration maintained constant, while the molar ratios of the two components varied. The adenine NH₂ resonance shifted at different molar fractions of [ionene-T]:[nBA], and [nBT]:[nBA] complexes and thymine NH chemical shift at different molar fractions of [ionene-A]:[nBT]. Fig. 2 demonstrates Job's plots for [ionene-A]:[nBT],

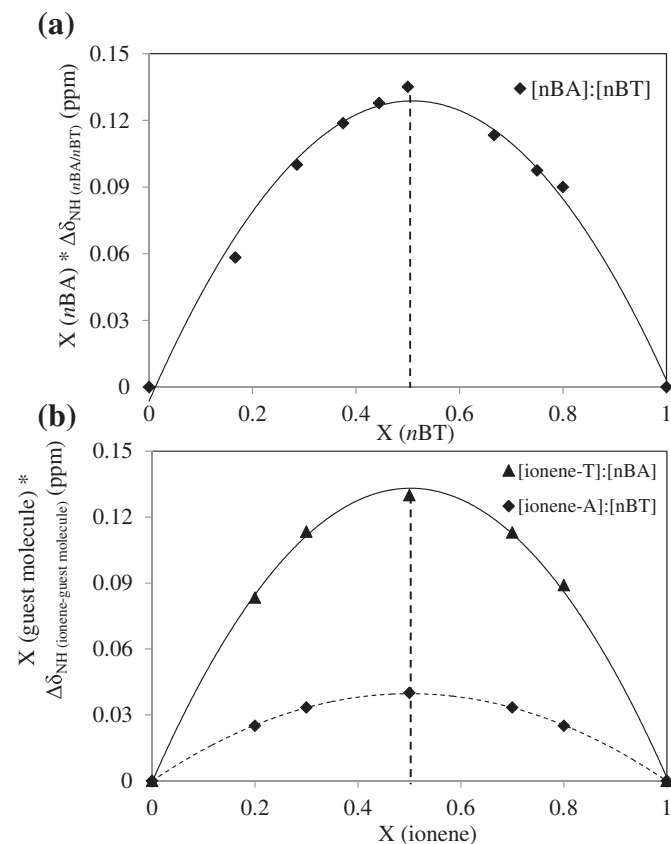


Fig. 2. Job's plot to determine the stoichiometry of (a) [nBT]:[nBA], (b) [ionene-T]:[nBA], and [ionene-A]:[nBT] complexes in CDCl₃.

[ionene-T]:[nBA], and [nBT]:[nBA]. The x-axis value of the parabolic maximum of the Job's plot represents the stoichiometry of the complex. All plots were symmetric and had a maximum at a 0.5 molar fraction, which confirmed that base pairing occurred in a 1:1 fashion. Therefore, a maximum concentration of the complexes formed at a 1:1 equimolar concentration of host and guest [28].

^1H NMR titration experiments in chloroform, which is a solvent that favors hydrogen bonding interactions due to the relatively low dielectric constant, determined the association constants (K_a) between the adenine and thymine nucleobases. Solutions of [ionene-A]:[nBT] complexes were prepared where the [nBT] concentration remained constant at 4 mM and the [ionene-A] concentration systematically increased from 4 mM to 16 mM. The position of the NH resonance of nBT in the complex shifted downfield (from 8.11 to 8.35 ppm) with an increase in [ionene-A] concentration. The curvature of chemical shift data with increasing adenine concentration remained consistent with typical ^1H NMR titration curves [29]. The change in chemical shift with complexation results from a faster exchange between associated and dissociated A-T complex on the NMR time scale [25,30].

The Benesi–Hildebrand model is a mathematical method to determine the association constant (K_a) from an NMR titration experiment. This model fits the nonlinear chemical shift data for a dimeric hydrogen bond association assuming the complex is formed in 1:1 stoichiometry [25,31]. The association constant (K_a) from the Benesi–Hildebrand analysis is calculated using the equation: $1/\Delta\delta = 1/(K_a\Delta\delta_{\text{max}}[\text{ionene-A}]) + 1/\Delta\delta_{\text{max}}$. The $\Delta\delta_{\text{max}}$ is the maximum change of the chemical shift of the thymine NH proton. The slope of the double reciprocal plot is $1/K_a\Delta\delta_{\text{max}}$ and the intercept is $1/\Delta\delta_{\text{max}}$. Fig. 3 demonstrates a typical nonlinear NMR titration curve of induced chemical shift versus solution concentration. Fitting of this data to the Benesi–Hildebrand method produced a linear, double reciprocal plot based on the association of A–T complex, which further confirmed the 1:1 stoichiometry (Fig. 3). The K_a for the supramolecular assembly of nBT and ionene-A was 94 M^{-1} , which was consistent with earlier reports on adenine–thymine base pair recognition ($10\text{--}100 \text{ M}^{-1}$ in CDCl_3) [28,32,33].

Similar ^1H NMR titration experiments were suitable for the [ionene-T]:[nBA] complex. The concentration of [nBA] was 4 mM, and we systematically increased the [ionene-T] concentration from 4 mM to 16 mM. The position of the NH_2 resonance of nBA in the complex shifted downfield (from 5.61 to 5.68 ppm) with an increase in [ionene-T] concentration. The linear fit to the Benesi–Hildebrand model also confirmed a 1:1 stoichiometry. Fig. 4 depicts the double reciprocal plot of Benesi–Hildebrand for the association of [ionene-T] and [nBA]. The K_a calculated from the slope of this plot is 130 M^{-1} .

For comparison, ^1H NMR titrations were performed with the nBA and nBT guest molecules. The association constant K_a based on the slope of the plot represented in Fig. 5 was 137 M^{-1} . Although the K_a values calculated for the three complexes are quite comparable and within acceptable range for adenine–thymine interaction, the similarity of K_a values of 130 M^{-1} for [ionene-T]:[nBA] and [nBA]:[nBT] with K_a of 137 M^{-1} for [ionene-A] in CDCl_3 . This presumably led to efficient accessibility of nucleobases and stronger association between nucleobase pairs in solution.

3.3. Thermal transitions

Upon discovering the complementary behavior of nucleobase-containing ionenes with guest molecules in solution, we investigated the solid state properties of 1:1 molar ratios of ionene complexes with small guest molecules. We studied the thermal properties of ionene-A, ionene-T, and their complexes to

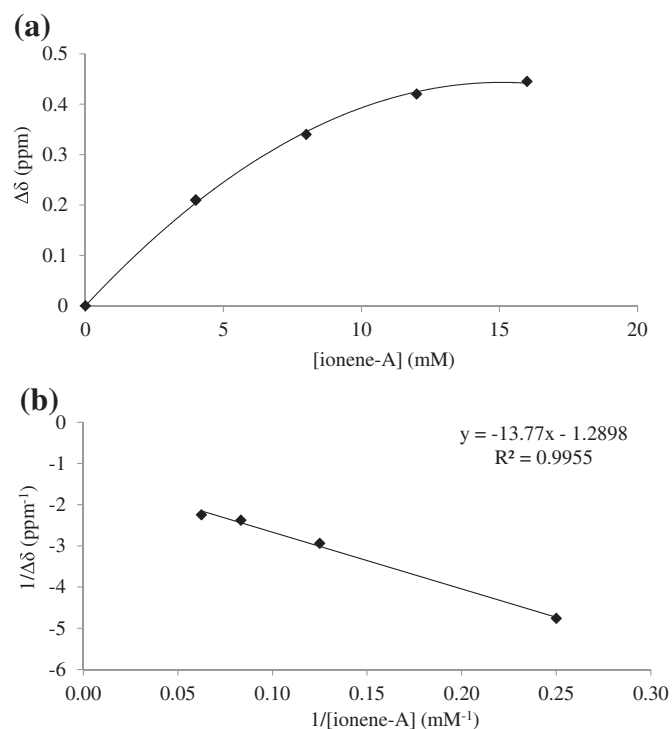


Fig. 3. (a) Nonlinear relationship between induced change for thymine NH chemical shift and ionene-A concentration, and (b) Benesi–Hildebrand plot of ionene-A and nBT guest molecule association in CDCl_3 .

understand the association of nucleobase pairs. All films were solution cast from chloroform and annealed at 100°C for 24 h *in vacuo*. DSC thermograms for the nucleobase-functionalized ionene homopolymers and complexes showed a single glass transition temperature at approximately -40°C . This transition

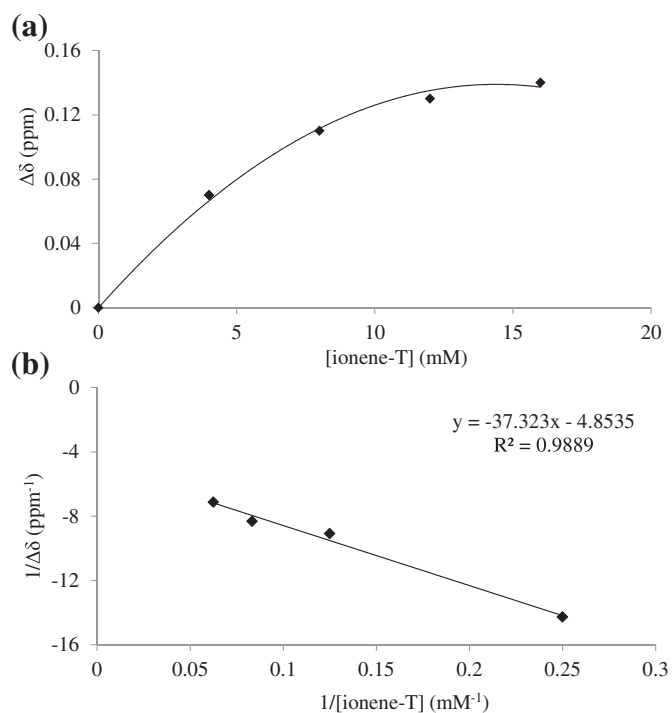


Fig. 4. (a) Nonlinear relationship between induced change for adenine NH_2 chemical shift and ionene-T concentration, and (b) Benesi–Hildebrand plot of ionene-T and nBA guest molecule association in CDCl_3 .

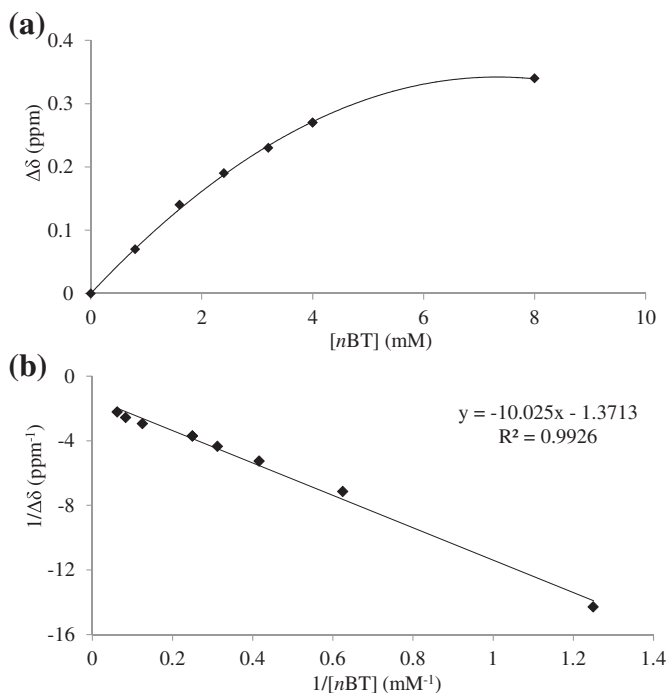


Fig. 5. (a) Nonlinear relationship between induced change for adenine NH_2 chemical shift and $n\text{BT}$ concentration, and (b) Benesi–Hildebrand plot of $n\text{BT}$ and $n\text{BA}$ guest molecule association in CDCl_3 .

corresponded to the T_g of the PEG soft segment (SS) (1000 g/mol) and confirmed a microphase separation of PEG SS from the ionic hard segment (HS). Since the nucleobases were incorporated into the hard phase, the hydrogen bonding interactions did not significantly influence the T_g of the SS. In the solution cast 1:1 blend of [ionene-A]:[$n\text{BT}$] and [ionene-T]:[$n\text{BA}$] from chloroform, the

Table 1
Thermal transitions of nucleobase-containing ionenes and their blends.

Sample	T_g ($^{\circ}\text{C}$) DSC	$T_{d5\%}$ ($^{\circ}\text{C}$) TGA
ionene-A	-36	246
ionene-T	-40	248
[ionene-A]:[$n\text{BT}$]	-31	243
[ionene-T]:[$n\text{BA}$]	-48	222

crystallization and melting peak of $n\text{BT}$ and $n\text{BA}$ were absent from the DSC thermograms (Fig. 6), and films were optically clear. Previously Mather and Long et al. [21] also showed that the addition of uracil-containing phosphonium salt to the adenine-containing triblock copolymers resulted in the disappearance of the phosphonium salt melting peak in the DSC thermograms. Thus, the absence of melting and crystallization peaks of the guest molecules indicated a well-defined hydrogen bonding interaction between the polymer and the guest molecule. Table 1 illustrates the thermal transitions of ionene homopolymers and ionene complexes.

3.4. Morphology

Atomic force microscopy (AFM) and X-ray scattering on annealed films of ionenes and ionene complexes ascertained the morphology. Fig. 7 includes AFM phase images of ionene-A and a 1:1 complex with $n\text{BT}$. The ionene-A revealed a microphase-separated morphology, the darker regions corresponded to the PEG SS (78 wt%) and the lighter regions corresponded to the harder ionic domains and heterocyclic nucleobases (22 wt%). Comparing the ionene segmented homopolymers with the blends showed a decreased phase contrast suggesting the disruption of the adenine-adenine hard phase through incorporation of complementary guest molecule. Fig. 8 illustrates the corresponding SAXS data. Due to the difference in electron density of the HS relative to the SS, a single peak was observed in the SAXS profile of ionene-A.

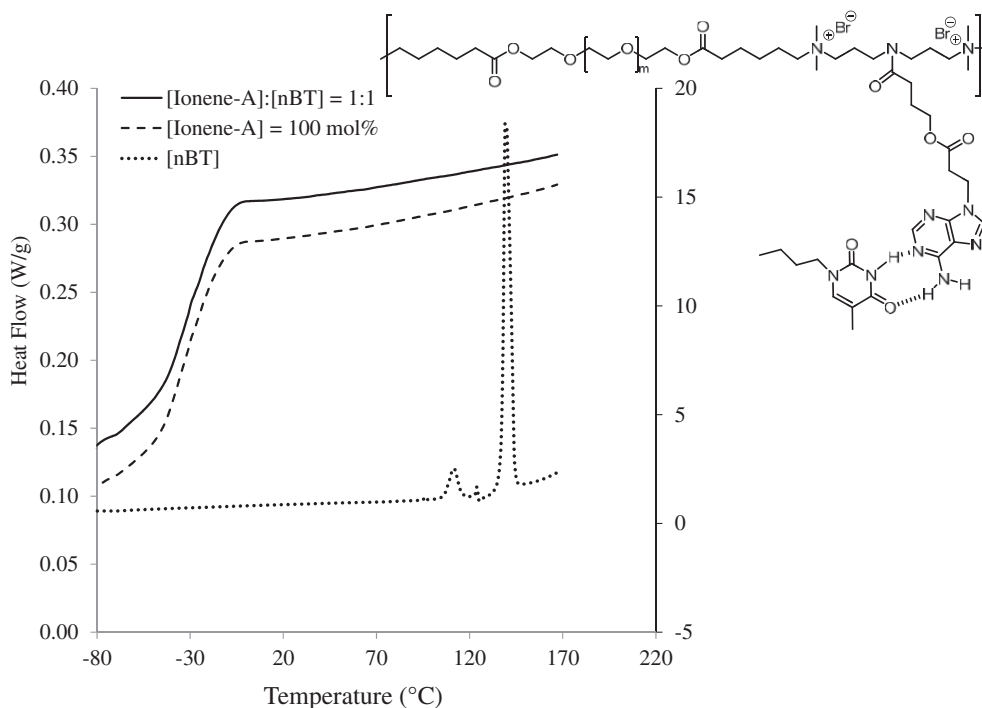


Fig. 6. DSC thermograms of ionene-A homopolymer and 1:1 complex with $n\text{BT}$. Second heating cycle is shown.

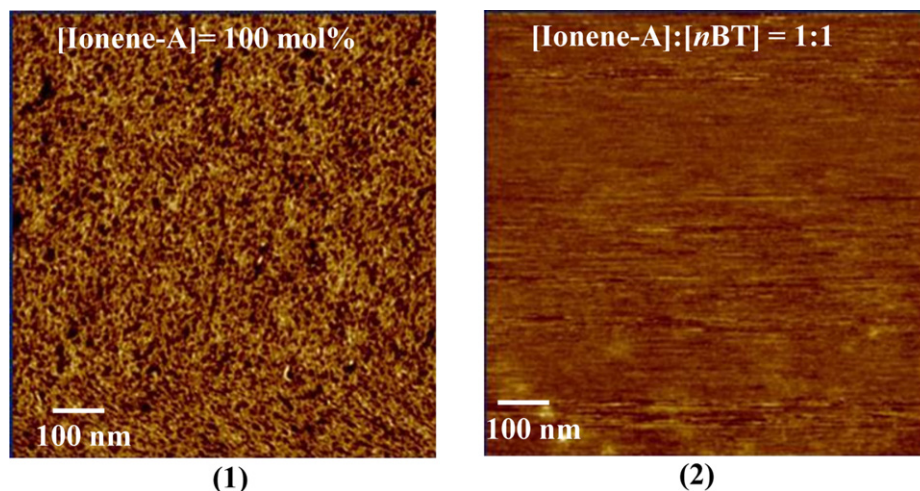


Fig. 7. AFM phase images of ionene-A (1) and 1:1 complex of [ionene-A]:[nBT] (2).

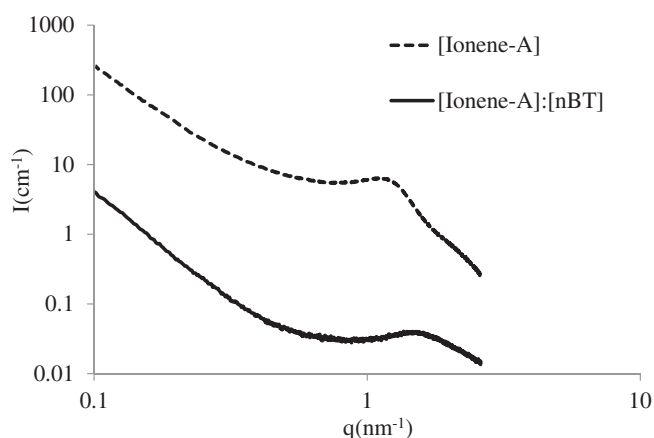


Fig. 8. SAXS data for ionene-A and 1:1 complex of [ionene-A]:[nBT].

The Bragg spacing, the distance between the ionic aggregates, of 5.75 nm for ionene-A was in agreement with our previous report on the 1K PPG-based ammonium ionenes having a Bragg spacing of 6.6 nm.[9] The SAXS data revealed that the addition of the nBT guest molecule resulted in a disruption of original morphology and led to a broad peak at shorter Bragg spacing of 4.62 nm.

4. Conclusions

Segmented nucleobase-containing ammonium ionenes were synthesized using post-polymerization functionalization. The blends of the ionene homopolymers with complementary nucleobase-containing guest molecules resulted in efficient hydrogen bonding interactions. Job's plots revealed a 1:1 stoichiometry for the hydrogen-bonded complexes of [ionene-A]:[nBT], [ionene-T]:[nBA], and [nBA]:[nBT]. The Benesi–Hildebrand analyses further confirmed the 1:1 complexation between ionene homopolymers and guest molecules, and the calculated association constants for [ionene-A]:[nBT], [ionene-T]:[nBA], and [nBT]:[nBA] complexes were 94, 130, and 137 M⁻¹ respectively. Since the nucleobases were incorporated into the hard phase, the hydrogen bonding interactions did not influence the T_g of the SS significantly. Therefore ionenes and complexes showed a single T_g at -40 °C corresponding to the T_g of PEG soft segment. The AFM and SAXS further confirmed a microphase-separated morphology for the

ionenes. AFM phase images showed a decrease in phase contrast with the incorporation of complementary guest molecules, and the SAXS revealed a broader peak at higher q values.

Appendix A. Supplementary data

Supplementary data related to this article can be found at <http://dx.doi.org/10.1016/j.polymer.2013.01.040>.

References

- [1] Lutz J-F, Thuenemann AF, Rurack K. *Macromolecules* 2005;38:8124.
- [2] Mather BD, Baker MB, Beyer FL, Berg MAG, Green MD, Long TE. *Macromolecules* 2007;40:6834.
- [3] Williams SR, Long TE. *Prog Polym Sci* 2009;34:762.
- [4] Ramirez SM, Layman JM, Long TE. *Macromol Biosci* 2009;9:1127.
- [5] Trukhanova ES, Izumrudov VA, Litmanovich AA, Zelikin AN. *Bio-macromolecules* 2005;6:3198.
- [6] Jacquet B, Lang G. Quaternized polymer for use as a cosmetic agent in cosmetic compositions for the hair and skin; 1980. US4217914A.
- [7] Narita T, Ohtakeyama R, Nishino M, Gong JP, Osada Y. *Colloid Polym Sci* 2000; 278:884.
- [8] Factor A, Heinsohn GE. *J Polym Sci, Part C Polym Lett* 1971;9:289.
- [9] Tamami M, Williams SR, Park JK, Moore RB, Long TE. *J Polym Sci, Part A Polym Chem* 2010;48:4159.
- [10] Tamami M, Salas-de ICD, Winey KI, Long TE. *Macromol Chem Phys* 2012; 213:965.
- [11] Cheng S, Zhang M, Dixit N, Moore RB, Long TE. *Macromolecules* 2012;45:805.
- [12] Lin IH, Cheng C-C, Yen Y-C, Chang F-C. *Macromolecules* 2010;43:1245.
- [13] Lo PK, Sleiman HF. *J Am Chem Soc* 2009;131:4182.
- [14] Spijker HJ, van DFL, van HJCM. *Macromolecules* 2007;40:12.
- [15] Lutz J-F, Pfeifer S, Chanana M, Thuenemann AF, Bienert R. *Langmuir* 2006; 22:7411.
- [16] Bazzi HS, Sleiman HF. *Macromolecules* 2002;35:9617.
- [17] McHale R, O'Reilly RK. *Macromolecules* 2012.
- [18] Xu H, Hong R, Lu T, Uzun O, Rotello VM. *J Am Chem Soc* 2006;128:3162.
- [19] Nair KP, Weck M. *Macromolecules* 2007;40:211.
- [20] Hemp ST, Hunley MT, Cheng S, DeMella KC, Long TE. *Polymer* 2012;53:1437.
- [21] Mather BD, Baker MB, Beyer FL, Green MD, Berg MAG, Long TE. *Macromolecules* 2007;40:4396.
- [22] Huang P-Q, Zheng X, Deng X-M. *Tetrahedron Lett* 2001;42:9039.
- [23] Lira EP, Huffman CW. *J Org Chem* 1966;31:2188.
- [24] Yamauchi K, Lizotte JR, Long TE. *Macromolecules* 2003;36:1083.
- [25] Fielding L. *Tetrahedron* 2000;56:6151.
- [26] Job P. *Ann Chim Appl* 1928;9:113.
- [27] Sahai R, Loper GL, Lin SH, Eyring H. *Proc Nat Acad Sci U S A* 1974;71:1499.
- [28] Nowick JS, Chen JS, Noronha G. *J Am Chem Soc* 1993;115:7636.
- [29] Karikari AS, Mather BD, Long TE. *Biomacromolecules* 2007;8:302.
- [30] Park T, Zimmerman SC. *J Am Chem Soc* 2006;128:11582.
- [31] Mesplet N, Morin P, Ribet J-P. *Eur J Pharm Biopharm* 2005;59:523.
- [32] Sivakova S, Bohnsack DA, Mackay ME, Suwanmala P, Rowan SJ. *J Am Chem Soc* 2005;127:18202.
- [33] Kyogoku Y, Lord RC, Rich A. *Biochim Biophys Acta, Nucleic Acids Protein Synth* 1969;179:10.